BRAIN
ORIGINAL ARTICLE

Defining the phenotypic spectrum of sporadic Creutzfeldt–Jakob disease MV2K: the kuru plaque type

Simone Baiardi,[1,2] Angela Mammana,[1] Sofia Dellavalle,[1] Marcello Rossi,[1] Veronica Redaelli,[3] Elisa Colaizzo,[4] Giuseppe Di Fede,[3] Anna Ladogana,[4] Sabina Capellari[1,2] and Piero Parchi[1,2]

The current classification of sporadic Creutzfeldt–Jakob disease identifies six major subtypes mainly defined by the combination of the genotype at polymorphic codon 129 (methionine/M or valine/V) of the prion protein gene and the type (1 or 2) of misfolded prion protein accumulating in the brain (e.g. MM1, MM2, MV1, MV2, etc.).

Here, we systematically characterized the clinical and histo-molecular features associated with the third prevalent subtype, the MV2 subtype with kuru plaques (MV2K), in the most extensive series collected to date. We evaluated neurological histories, cerebrospinal biomarkers, brain MRI and EEG results in 126 patients. The histo-molecular assessment included misfolded prion protein typing, standard histologic staining and immunohistochemistry for prion protein in several brain areas. We also investigated the prevalence and topographic extent of coexisting MV2-cortical features, the number of cerebellar kuru plaques and their effect on clinical phenotype.

Systematic regional typing revealed a western blot profile of misfolded prion protein comprising a doublet of 19 and 20 kDa unglycosylated fragments, with the former more prominent in neocortices and the latter in the deep grey nuclei. The 20/19 kDa fragment ratio positively correlated with the number of cerebellar kuru plaques. The mean disease duration was exceedingly longer than in the typical MM1 subtype (18.0 versus 3.4 months). Disease duration correlated positively with the severity of pathologic change and the number of cerebellar kuru plaques. At the onset and early stages, patients manifested prominent, often mixed, cerebellar symptoms and memory loss, variably associated with behavioural/psychiatric and sleep disturbances. The cerebrospinal fluid prion real-time quaking-induced conversion assay was positive in 97.3% of cases, while 14-3-3 protein and total-tau positive tests were 52.6 and 75.9%. Brain diffusion-weighted MRI showed hyperintensity of the striatum, cerebral cortex and thalamus in 81.4, 49.3 and 33.8% of cases, and a typical profile in 92.2%. Mixed histotypes (MV2K + MV2-cortical) showed an abnormal cortical signal more frequently than the pure MV2K (64.7 versus 16.7%, $P = 0.007$). EEG revealed periodic sharp-wave complexes in only 8.7% of participants.

These results further establish MV2K as the most common 'atypical' subtype of sporadic Creutzfeldt–Jakob disease, showing a clinical course that often challenges the early diagnosis. The plaque-type aggregation of the misfolded prion protein accounts for most of the atypical clinical features. Nonetheless, our data strongly suggest that the consistent use of the real-time quaking-induced conversion assay and brain diffusion-weighted MRI allows an accurate early clinical diagnosis in most patients.

1 IRCCS Istituto delle Scienze Neurologiche di Bologna, 40139 Bologna, Italy
2 Department of Biomedical and Neuromotor Sciences (DIBINEM), University of Bologna, 40138 Bologna, Italy
3 Neuropathology Unit, Fondazione I.R.C.S.S. Istituto Neurologico Carlo Besta, 20133 Milan, Italy
4 Department of Neuroscience, Istituto Superiore di Sanità, 00161 Rome, Italy

Received November 01, 2022. Revised January 28, 2023. Accepted February 22, 2023. Advance access publication March 8, 2023

Correspondence to: Professor Piero Parchi
IRCCS Istituto delle Scienze Neurologiche
Ospedale Bellaria, Via Altura 1/8, 40139, Bologna, Italy
E-mail: piero.parchi@unibo.it

Keywords: prion protein; RT-QuIC; scrapie; strain; seeding assay

Introduction

The broad phenotypic heterogeneity of sporadic Creutzfeldt–Jakob disease, the most common human prion disease, depends on prion protein (PrP) gene (*PRNP*) sequence variations and the proprieties of the abnormal PrP (PrP^{Sc}) aggregates accumulating in the brain. The primary genetic determinant is a methionine (M)/valine (V) polymorphism at codon 129 of *PRNP*, leading to three possible combinations MM, MV or VV.[1] The second molecular determinant is the PrPSc proteinase K-resistant core fragment size, which identifies two main unglycosylated fragments, type 1 with a relative molecular mass of 21 kDa and type 2 of 19 kDa.[2] The codon 129 genotype-PrP^{Sc} type combination determines six major disease subtypes, with minor exceptions.[3] They include the MM1 and MV1 merging into a single subtype and the MM2 splitting into two clinicopathological subtypes with prominent cortical (MM2C) or thalamic (MM2T) distribution of pathologic changes. As a result, the current classification of sporadic Creutzfeldt–Jakob disease identifies the following six main subtypes: MM/MV1, MM2C, MM2T, VV1, VV2 and MV2.[3] Experimental transmissions in syngeneic hosts, demonstrating that five out of six subtypes behave as distinct prion strains, supported this classification strongly.[4] As the only exception, VV2 and MV2K converged to a single strain named V2 because it transmits more efficiently in the presence of 129V than 129M.[4]

The prototype of V2 infection is the VV2 subtype, also known as 'cerebellar' or Brownell–Oppenheimer variant, characterized by short duration, early and prominent ataxia, and an ascending intracerebral spreading that results in late involvement of the cerebral cortex and dementia.[5]

In heterozygotes (MV2K subtype), the V2 strain converts both PrP^{C} isoforms (i.e. with valine or methionine at codon 129) but with a reduced replication efficiency.[4,6] This leads to a more prolonged clinical course, a more widespread CNS involvement at clinical onset, and a reduced response of neurodegenerative diagnostic biomarkers in biofluids compared to the VV2 phenotype.[3,7,8] Moreover, the conversion of PrP^{C}-129M seems to be fundamental for PrP^{Sc} aggregation in the form of kuru plaque, as elegantly demonstrated by experimental traceback transmissions, which identified the V2 strain as responsible for iatrogenic Creutzfeldt–Jakob disease 129MM phenotype with kuru plaques.[9] PrP^{Sc} deposition as extracellular amyloid plaques rather than diffuse membrane-associated aggregates could be another determinant of the less aggressive disease phenotype, given the reduced neurotoxicity of these PrP^{Sc} deposits.

It is also noteworthy that, in patients carrying MV, the V2 strain may coexist with other strains associated with different conformations of PrP^{Sc}-129M (e.g. M1, M2C), leading to mixed histotypes (e.g. MV2K + MV2C, MV2K + MV1), which further contributes to phenotypic heterogeneity. Additionally, initial evidence from the topographic distribution of mixed histotypes suggests that allele-specific conversion by prion strains might be region dependent.[10]

Despite the evidence provided by animal models, the effective contribution of specific molecular (strain) features on the clinicopathological phenotype of this peculiar disease subtype is not well known. MV2K represents the third most common sCJD subtype in Western countries while having a relatively low prevalence in Asia due to the rarity of the codon 129V *PRNP* allele in these populations.[10–13]

Here, we have comprehensively characterized the histo-molecular features of MV2K, aiming to define the determinants of the 'unusual' clinical phenotype associated with this sCJD subtype. Additionally, we examined the results of diagnostic investigations [EEG, MRI, CSF 14-3-3 and real-time quaking-induced conversion (RT-QuIC) assay] and other surrogate biomarkers in both CSF and plasma of potential utility for diagnostic and severity stratification purposes.

Materials and methods

Patients and selection criteria

We included 126 patients with sporadic Creutzfeldt–Jakob disease carrying the MV genotype at *PRNP* polymorphic codon 129. All patients had a comprehensive clinical assessment, being hospitalized in a Neurology Department at least once during the disease course. Eighty-seven received a 'definite' diagnosis of sporadic Creutzfeldt–Jakob disease MV2K (or MV2K + 2C) by post-mortem brain tissue studies according to molecular and histopathological consensus criteria.[10,14,15] Of the 87 patients, 57 were referred to the Neuropathology Laboratory (NP-Lab) at the Institute of Neurological Science of Bologna, Italy (from 2000 to 2021), 12 to the Foundation IRCCS, Carlo Besta Institute of Neurology, Milan, Italy (from 1994 to 2016), and 18 were part of a previously published case series.[3] The remaining 39 (all from the NP-Lab) fulfilled the current diagnostic for 'probable' sporadic Creutzfeldt–Jakob disease and tested positive by the CSF prion RT-QuIC assay. To define clinical criteria distinguishing probable MV2K from MV1 and MV2C (i.e. two rarer subtypes associated with codon 129 heterozygosity), we reviewed all definite MV1 ($n = 22$) and MV2C ($n = 3$) from a consecutive series of 548 sporadic Creutzfeldt–Jakob disease cases submitted at the NP-Lab between 2000 and 2021. In line with the current literature,[3,10] MV1 showed a significantly shorter disease duration than MV2K (Supplementary Table 1). Moreover, none of the MV2C participants presented symptoms of cerebellar or nigrostriatal involvement within 12 months from disease onset, a finding consistent with the dominant cortical pathology and relative sparing of the cerebellum characterizing this subtype.[10] Therefore, we used the following conservative criteria to define a case as 'probable MV2K': (i) disease duration >8 months (i.e. the mean disease duration of MV1 cases plus two standard deviations) and (ii) clinical evidence of cerebellar and/or nigrostriatal involvement within 6 months from the onset. All 39 probable participants in the MV2K group fulfilled the previously mentioned criteria.

Molecular genetic analyses

To rule out pathogenic *PRNP* mutations and confirm codon 129 heterozygosity, we performed PCR amplification and sequencing of genomic DNA from all included subjects, according to a previously published protocol.[16]

Protein studies

We prepared the brain homogenates and performed PrP^{Sc} typing by western blot according to established methods.[14,17] Briefly, samples were run in a 15 cm long separating gel, transferred to Immobilon-P membranes (Millipore) and probed overnight with the monoclonal antibody 3F4 (1:30 000 working dilution). The immunoreactive signal was visualized by enhanced chemiluminescence (Immobilon Western, Millipore) on a LAS 3000 camera (Fujifilm).

To evaluate in-depth the regional variability of PrP^{Sc} typing, we performed immunoblots in samples from 22 regions (Supplementary Table 2) in a subgroup of 25 patients. Western blot signals, including the ratio of unglycosylated PrP^{Sc} isoforms (19 and 20 kDa fragments), were measured semiquantitatively by densitometry using AIDA software (Raytest, Germany).

Neuropathology

The brains of 84 participants were obtained by autopsy and handled according to a standardized procedure.[10] Briefly, either one-half (right hemisphere) or selected coronal tissue sections, including all major brain structures and nuclei, were frozen immediately and stored in sealed bags at −80°C. The remaining tissue (in most cases from the left hemisphere) was fixed in formalin and was used for neuropathological examination and PrP immunohistochemistry.

Histopathological assessment

Standard routine histopathological staining was performed in all 84 brains. Additionally, a semiquantitative evaluation of grey matter spongiosis and gliosis was carried out in 67 cases by analysing haematoxylin eosin-stained sections obtained from 20 brain regions (Supplementary Table 2). The same experienced neuropathologist (P.P.) rated spongiosis on a 0–4 scale (not detectable, mild, moderate, severe and status spongiosis) and gliosis on a 0–3 scale (not noticeable, mild, moderate and severe). Then, a lesion profile for each patient was obtained by averaging the two scores.

Prion protein immunohistochemistry

We performed PrP immunohistochemistry on formalin-fixed and paraffin-embedded blocks of the areas selected for histopathologic examination. PrP immunohistochemistry was carried out using the monoclonal antibody 3F4 (1:400, Signet Labs) as described.[18] PrP deposits were described as diffuse or synaptic, perivacuolar, coarse or patchy, plaque-like and kuru plaques. To evaluate the co-occurrence of different histotypes within the same brain, we investigated the regional distribution of PrP deposition in the following brain regions: frontal ($n = 67$), temporal ($n = 57$), parietal ($n = 57$) and occipital (both calcarine sulcus and lateral occipital gyrus, $n = 59$ and $n = 54$, respectively) neocortices, striatum ($n = 63$), thalamus ($n = 58$), hypothalamus ($n = 45$), midbrain ($n = 45$), pons ($n = 40$), medulla ($n = 42$) and cerebellum ($n = 63$).

We classified the mixed phenotypes according to both PrP^{Sc} typing and histotyping data. We only detected mixed cases in which MV2K was the dominant phenotype with 2C as a secondary component (i.e. MV2K + 2C). These cases were characterized by large confluent vacuoles and a perivacuolar pattern of PrP deposition at immunohistochemistry (i.e. the hallmarks of the MM/MV2C subtype).

Quantification of cerebellar kuru plaques

For this purpose, sections of the cerebellum at the level of the dentate nucleus were processed for periodic acid-Schiff staining. Two operators (S.B. and P.P.) separately evaluated and manually counted periodic acid-Schiff-positive plaques in 10 cerebellar folia of each case at ×200 magnification. Both operators reviewed all discordant cases (i.e. total amount >5 plaques) to reach an agreement. A kuru plaque score was calculated, representing the mean number of kuru plaques in each cerebellar folium.

Assessment of neurodegenerative co-pathologies

In 49 brains, we performed immunohistochemistry with antibodies specific for Aβ (4G8, dilution 1:5000, Signet Labs), p-tau (AT8, dilution 1:200, Immunogenetics) and α-synuclein (LB509, dilution 1:100, Thermo Fisher Scientific), using several brain regions, mainly following established consensus criteria.[19–21]

Clinical analysis

We reviewed the clinical chart for each patient's neurological symptoms and signs at the onset and during the disease course. We defined as 'onset symptom(s)' the first neurological disturbance(s) complained by the patient at disease onset, and as 'early symptoms' those reported in the first 6 months from onset, a time representing approximately the first third of the average disease duration in MV2K subtype. Moreover, we calculated the mean time of appearance of all reported symptoms/signs from disease onset grouped according to the following categories: ataxia/cerebellar, psychiatric, myoclonus, sensory/peripheral nervous system, visual, oculomotor, pyramidal, parkinsonism, cognitive (single-domain), dementia and akinetic mutism. Disease duration was calculated from the presentation of neurological signs to death. Finally, for each case, we searched for all available information concerning the alternative diagnosis taken into consideration at the time of neurological assessment.

Diagnostic investigations

CSF analyses

Prion RT-QuIC

Prion RT-QuIC using full-length [residues 23–231, previous QuIC (PQ)-CSF] or truncated [residues 90–231, improved QuIC (IQ)-CSF] hamster recombinant PrP as substrate was performed as previously described.[22,23]

Protein 14-3-3

Protein 14-3-3 was detected semiquantitatively by western blot as described.[22] Alternatively, we measured 14-3-3 gamma isoform using a commercially available enzyme-linked immunosorbent assay (ELISA) assay kit (Circulex 14-3-3 gamma ELISA kit, MBL) according to the manufacturer's instructions. According to our in-house cut-off, we considered 'positive' the 14-3-3 assay with values >23 400 AU/ml.[24]

Diffusion-weighted MRI

We reviewed all available cerebral MRI results focusing on studies including fluid-attenuated inversion recovery (FLAIR) and/or diffusion-weighted imaging (DWI) sequences. MRIs without DWI/FLAIR sequences were not analysed further. Specifically, we searched for hyperintensities on T_2-FLAIR and/or DWI sequences in eight brain areas, namely temporal, parietal and occipital cortices, striatum (caudate and putamen nuclei), thalamus, hippocampus, insula and cingulate gyrus. We also evaluated the timing of MRI studies after the onset of symptoms. According to current

diagnostic criteria for sporadic Creutzfeldt–Jakob disease,[25] we considered a 'typical' positive finding the presence of hyperintensities on T_2-FLAIR and/or DWI in at least two cortical regions (temporal, parietal and occipital cortices) and/or the striatum.

EEG

EEG recordings were reviewed, and abnormal traces were classified as follows: (i) diffuse nonspecific slowing; (ii) paroxysmal discharges; and (iii) periodic sharp-wave complexes (PSWCs).[26] When multiple EEG recordings were available for review, we assigned the highest degree of severity according to the following rule: PSWCs > paroxysmal discharges > slowing.

Other surrogate biomarkers of neurodegeneration

CSF total tau (t-tau) was measured by sandwich ELISA (INNOTEST, Fujirebio) or by automated chemiluminescent enzyme immunoassay on the Lumipulse G600II platform (Fujirebio). In CSF, neurofilament light chain (NfL) was quantified by a validated commercial ELISA (NfL ELISA kit, IBL),[27] while plasma NfL was measured with the SiMOA NF-light advantage kit on a SiMOA SR-X analyser platform (Quanterix).

Statistical analysis

Statistical analysis was performed using GraphPad Prism 8 (GraphPad Software, La Jolla, CA, USA). Depending on the data distribution, the Mann–Whitney U-test or the two-tailed Student t-test was used, as appropriate, to test differences between two groups of continuous variables. The one-way ANOVA or Kruskal–Wallis test (followed by Bonferroni's or Tukey's *post hoc* tests) was used for multiple group comparisons. The chi-square test and Fisher's exact test were adopted for categorical variables. The Spearman bivariate test was used to evaluate the strength of the correlation between clinical and histo-molecular findings. Hypothesis testing was two-sided, and $P \leq 0.05$ were considered statistically significant.

Finally, to identify the best combination between clinical features and ancillary tests, allowing an accurate diagnosis, we calculated the diagnostic sensitivity of different associations of biomarkers and clinical characteristics at the time of CSF collection and after the whole disease course. For this purpose, we analysed 48 MV2K cases (19 definite and 29 probable) with all biomarkers available. The definitions of the combination criteria are reported in Supplementary Fig. 1.

Ethics statement

Data collection of clinically suspected cases is an integral part of the National Creutzfeldt–Jakob disease surveillance study, which was approved by the Ethics Committee of the Istituto Superiore di Sanità (CE-ISS 09/266 on 29 May 2009).

Data availability

The data supporting this study's findings are available from the corresponding author upon reasonable request.

Results

Estimated prevalence

In the neuropathologic cohort of the NP-Lab (2000–2021), including 548 Caucasian individuals with definite sporadic Creutzfeldt–Jakob disease, MV2K (pure or mixed) was the third most prevalent subtype accounting for 10.6% of cases.

Molecular genetic analyses

None of the participants carried pathogenic mutations in the *PRNP* open reading frame. All patients carried the MV genotype at codon 129.

Protein studies

As previously described,[10,17] the immunoblot profile of proteinase K-resistant PrP^{Sc} showed an unglycosylated fragment migrating at 19 kDa (type 2) in all definite participants, associated with a variable relative amount of a second peptide migrating at 20 kDa depending on the brain region analysed (Fig. 1). The 19 kDa fragment was dominant in the neocortices in most cases (20/25, 80%) (Fig. 1A). In contrast, we found a dominant 20 kDa band or iso-intensity between bands in subcortical regions including striatum (23/25 cases, 92%), thalamus (22/25, 88%), hippocampus (22/25, 88%) and brainstem (18/20, 90%). The cerebellum showed the highest variability, with a dominant 20 kDa or an iso-intensity pattern in 16 patients (64%) and a dominant 19 kDa band in nine (36%) (Fig. 1B). Further analysis of all cases with frozen tissue available from the neocortex (middle temporal gyrus), medial thalamus and cerebellar hemisphere confirmed the results obtained in the exploratory group. Specifically, the 20 kDa/iso-intensity pattern was prevalent in the thalamus (55/60, 91.7%) and cerebellum (43/56, 76.7%), while the 19 kDa fragment predominated in the temporal cortex (45/63, 71.4%). As in other sporadic Creutzfeldt–Jakob subtypes, the analysis of PK-resistant PrP^{Sc} glycoforms (i.e. glycoform ratio) generally revealed a predominant monoglycosylated isoform. However, there was some heterogeneity among the areas analysed (Supplementary Table 3), probably reflecting the stage and severity of pathologic changes related to disease duration, the ratio between the 19/20 kDa bands and possibly regional differences in PrP^{C} glycosylation.

Neuropathology

Severe spongiform change, gliosis and neuronal loss affected the striatum, thalamus and entorhinal cortex, whereas other limbic structures, such as the hippocampus, amygdala and cingulate gyrus, the hypothalamus and the cerebellum showed moderate changes. Of note, despite the invariable involvement, the latter showed less severe changes than the cerebellum of VV2 brains (Fig. 2A). The brainstem was consistently affected by mild to moderate pathologic changes. Spongiform change mainly involved the substantia nigra and periaqueductal grey (midbrain), the grey matter next to the locus coeruleus (pons) and anterior to the fourth ventricle (medulla) (Supplementary Fig. 2).

All neocortices showed mild to severe pathologic change, slightly more pronounced in the frontal cortex, depending on the disease duration. A more severe neocortical pathology characterized the individuals with a prolonged clinical course (Fig. 2B). In contrast, the intensity of pathologic change in subcortical nuclei and limbic cortices was comparable between short- and long-duration cases, suggesting these regions were involved earlier during the disease course. Interestingly, we found higher pathologic scores in the temporal neocortex in the brains that showed a dominant 20 kDa PrP^{Sc} unglycosylated fragment compared with those with a predominant 19 kDa band (mean score 2.5 ± 1.1 versus 1.4 ± 0.8, $P = 0.004$). Spongiform change comprised intermediate size, non-confluent

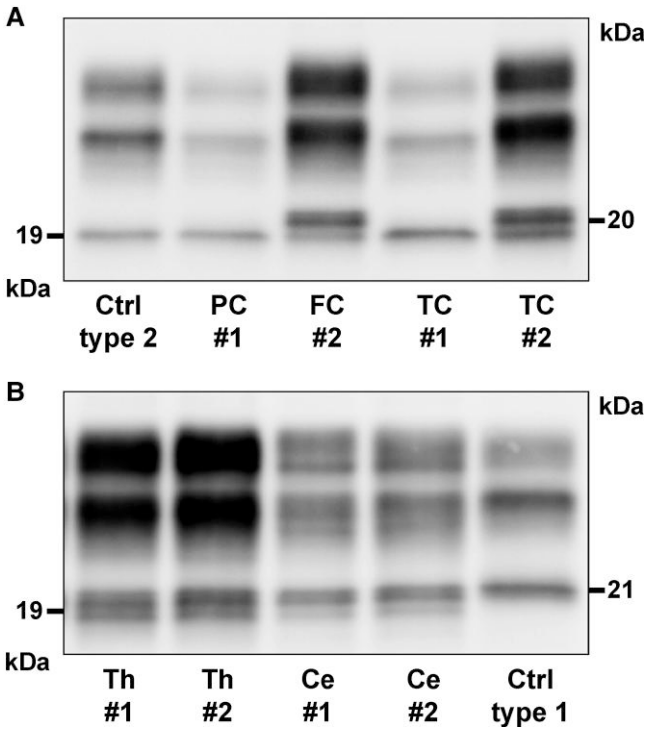

Figure 1 Regional immunoblot profiles of proteinase K–resistant PrP^{Sc} fragments in two representative sporadic Creutzfeldt–Jakob disease MV2K cases (#1 and #2). (**A**) Western blot profile in neocortices showing a dominant 19 kDa (type 2) unglycosylated band in Case #1 and, conversely, a dominant 20 kDa fragment in Case #2. (**B**) Immunoblot of thalamus showing a similar intensity of 19 and 20 kDa bands and a dominant 20 kDa fragment in the cerebellum (vermis) of both cases. Immunoblots are probed with the mAb 3F4.

vacuoles and often showed a striking laminar distribution in the deeper layers (IV-VI) of neocortices (Fig. 3A). The latter finding was particularly evident in cases with shorter duration showing less severe pathologic changes.

PrP immunochemistry revealed amyloid (kuru type) plaques and plaque-like deposits in the granular layer of the cerebellum in all cases (Table 1 and Fig. 3B and C).

In the cerebellum, kuru plaques were seen prominently within the internal granular cell layer, at the junction with the Purkinje cell layer, and, in most cases, near the white matter. Kuru plaques also extended to the molecular layer proportionally with the overall number of cerebellar plaques (Figs 2C and 3D). In a subgroup of cases (i.e. all with high cerebellar kuru scores), plaques were also detected in the neocortex, thalamus and striatum (Table 1 and Figs 2D and 3E). The number of kuru plaques was associated with disease duration (Fig. 2E). There was also a trend towards a positive correlation with the severity of pathologic changes in the cerebellum (rho = 0.261, $P = 0.054$). Additionally, cerebellar kuru scores were higher in individuals with the dominant 20 kDa unglycosylated PrP^{Sc} fragment than in those with the dominant 19 kDa band in the cerebellum (Fig. 2F).

Plaque-like deposits were invariably present in the cerebellar granular layer, thalamus, striatum and brainstem, as in most neocortices. However, this pattern of PrP deposition was more abundant in the cerebellum and subcortical structures (e.g. thalamus, putamen and substantia nigra) than in the neocortex and in cases with higher cerebellar kuru scores. As a general observation, plaque-like deposits were larger in the cerebellum than in the striatum and brainstem. In neocortices, PrP typically accumulated in the form of delicate, punctate/granular synaptic deposits, often surrounding the neuronal perikarya and dendrites (perineuronal distribution) (Fig. 3F) and to a lesser extent with a plaque-like pattern that largely colocalized with spongiform change in the deeper layers (Fig. 3G). In the hypothalamus, the pattern of PrP deposits was either small plaque-like (in most cases), synaptic (sometimes assuming a perineuronal distribution), or both (Supplementary Fig. 3).

In the neocortices of a subgroup of cases (24/67, 35.8%), we also observed large confluent, grape-like vacuoles associated with coarse PrP deposits surrounding vacuoles (perivacuolar distribution) (Fig. 3H and I). These features, virtually indistinguishable from those observed in MM2C, were mixed with those of 'pure' MV2K. Accordingly, we classified these cases as mixed MV2K + 2C histotype. The M2C showed a spatial distribution with a posterior (maximum extent in the occipital cortex) to anterior (minimum in the frontal cortex) gradient (Fig. 2G), although in seven cases (29.2%), all neocortices were affected. Nonetheless, the comparison of lesion profiles of MV2K and MV2K + 2C revealed only minor differences, limited to a slightly lower severity of pathologic change in the hippocampus and cerebellum in the mixed histotype (Fig. 2H). The cerebellar kuru score was significantly lower in MV2K + 2C than in pure MV2K (Fig. 2I). Moreover, according to the typical MM2C lesion profile, we found PrP perivacuolar deposits in the striatum in 16.7% of cases and occasionally in the thalamus. Finally, there were large PrP patches focally in the molecular layers of the cerebellum in two MV2K + 2C, a pattern consistent with long-duration MM2C (Fig. 3J).

Alzheimer's disease-related pathologic changes (ADRC) were found in 31 of the 49 brains analysed (63.1%). In 26 cases, ADRC were mild (low ABC score),[28] while four presented intermediate scores and one a high score. Additionally, seven participants (14.3%) were diagnosed with primary age-related tauopathy (four probable, three possible).[29] Cerebral amyloid angiopathy involving large parenchymal and meningeal vessels was observed in 11 brains (22.4%). The severity of ADRC was similar between MV2K and MV2K + 2C cases but with a trend towards a more widespread Aβ pathology in the latter group (Thal phase ≥3 42.9% versus 21.4%, $P = 0.129$).

As previously reported,[22] we detected a prion-related secondary tauopathy independent from ADRC, characterized by dot- or stub-like positive immunoreactive structures, probably representing delicate neurites, in the neocortices, striatum, thalamus and cerebellum (molecular and Purkinje cell layers) of MV2K individuals showing mild to moderate neuropathologic changes (Fig. 3K). In these cases, tau immunoreactivity colocalized mostly with spongiform change in the grey matter. Minimal or no tau immunoreactivity was seen when neuronal loss and gliosis were severe and in the cases with status spongiosus.

Incidental Lewy body pathology spatially restricted to the brainstem was detected in three cases (6.1%) (Braak stage 1 in two cases, stage 3 in one).

Sparse Hirano bodies were found in the hippocampus of 12 out of 26 cases (46.2%) with no evidence of tau-neurofibrillary pathology.

Clinical features

Among the 126 examined cases, the female: male ratio was 1.29:1 (71 female, 55 male), the mean age at clinical onset was 64.7 ± 9.9 years (range 35–85) and the mean disease duration 18.0 ± 11.7 months (range 2–155). Cases belonging to the MV2K

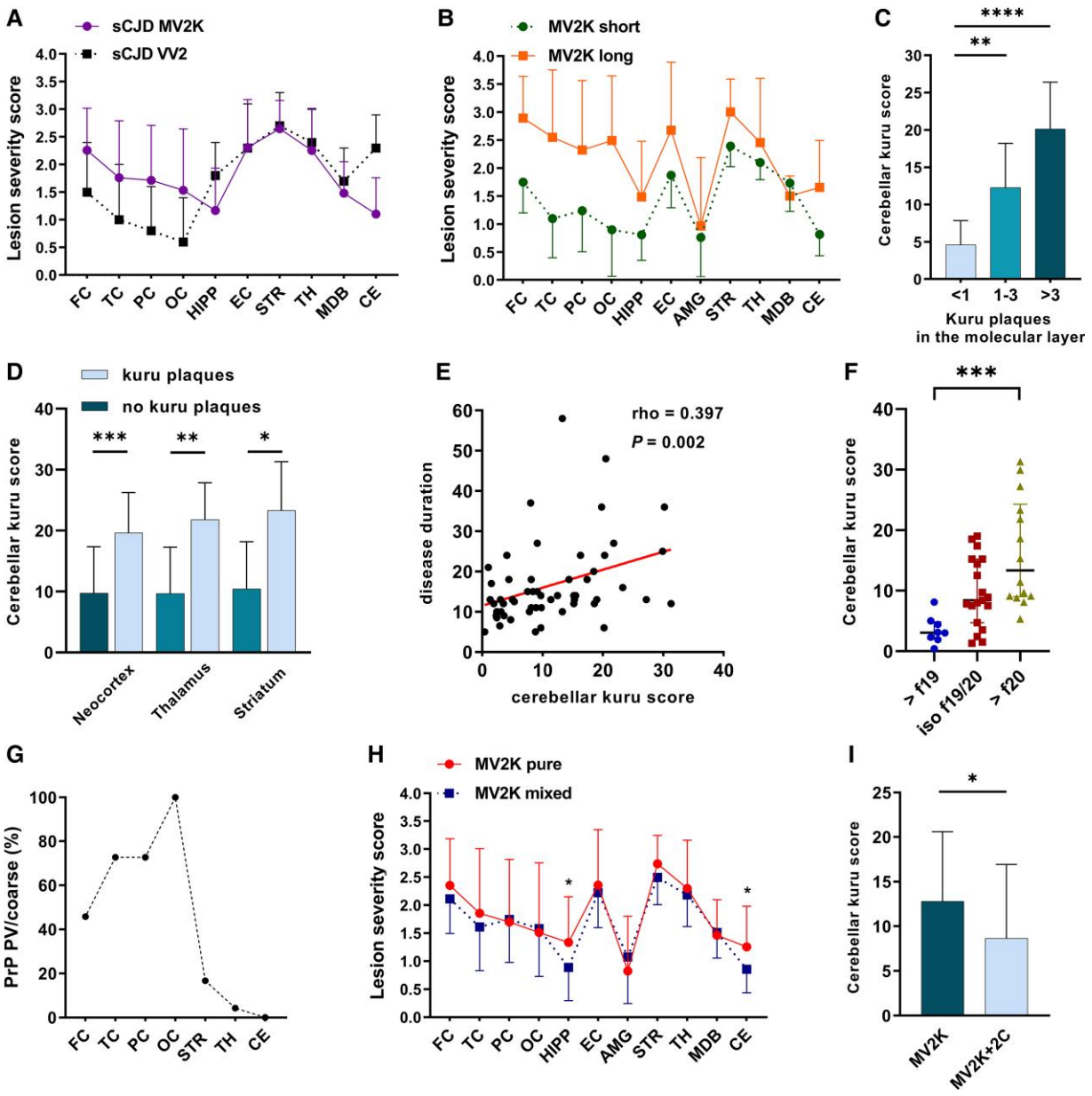

Figure 2 Relevant histo-molecular features and correlations in sporadic Creutzfeldt–Jakob disease MV2K subtype. (**A**) Comparison between lesion profiles of sporadic Creutzfeldt–Jakob disease MV2K and VV2. (**B**) Lesion profiles of MV2K with long (>18 months) and short (<9 months) disease duration. (**C**) Relationship between kuru plaque load in the cerebellar molecular layer and total amount in the cerebellum. (**D**) Relationship between cerebellar kuru plaque score and occurrence of kuru plaques outside the cerebellum. (**E**) Correlation between cerebellar kuru plaque score and disease duration. (**F**) Relationship between prominent unglycosylated PrP^{Sc} fragment size and cerebellar kuru score. (**G**) Spatial distribution of PrP perivacuolar (PV)/coarse deposits in MV2K + 2C phenotype. (**H**) Lesion profiles of pure MV2K and mixed MV2K + 2C phenotypes. (**I**) Comparison of cerebellar kuru score in pure and mixed phenotypes. (**A**, **B** and **H**) Data are expressed as mean and 95% confidence interval (bars). (**C**–**F**) Kuru scores represent the mean number of kuru per cerebellar folium. In **F**, >f19 = dominant 19 kDa fragment; iso f19/20 = iso-intensity between 19 and 20 kDa fragments; >f20 = dominant 20 kDa fragment. FC = frontal cortex; TC = temporal cortex; PC = parietal cortex; OC = occipital cortex; HIPP = hippocampus; EC = entorhinal cortex; AMG = amygdala; STR = striatum; TH = thalamus; MDB = midbrain; CE = cerebellum. $^{*}P \leq 0.05$, $^{**}P \leq 0.01$, $^{***}P \leq 0.001$, $^{****}P \leq 0.0001$.

+ 2C group were older than those of pure MV2K (68.2 ± 10.8 versus 62.1 ± 10.0 years, $P = 0.012$) (Supplementary Table 4). Clinical findings did not significantly differ between definite and probable cases, but for a higher prevalence of oculomotor disturbances in the former group (31.0 versus 12.9%, $P = 0.03$) (Supplementary Table 5).

Illness presentation was typically characterized by instability while walking or standing, often associated with various cognitive deficits, including impaired memory, poor attention and confusion, and a wide range of behavioural/psychiatric symptoms (Table 2 and Fig. 4). In about 20% of patients, gait disturbance occurred alone at disease onset, while memory loss was the most frequent isolated cognitive presentation. Besides gait unsteadiness, other presenting symptoms suggesting cerebellar involvement included vertigo, dysarthria and limb incoordination. Sleep complaints, including excessive sleepiness or insomnia, enacted dream behaviour and circadian rhythm misalignment, were reported by ~10% of patients at the onset but never as isolated symptoms. In five subjects,

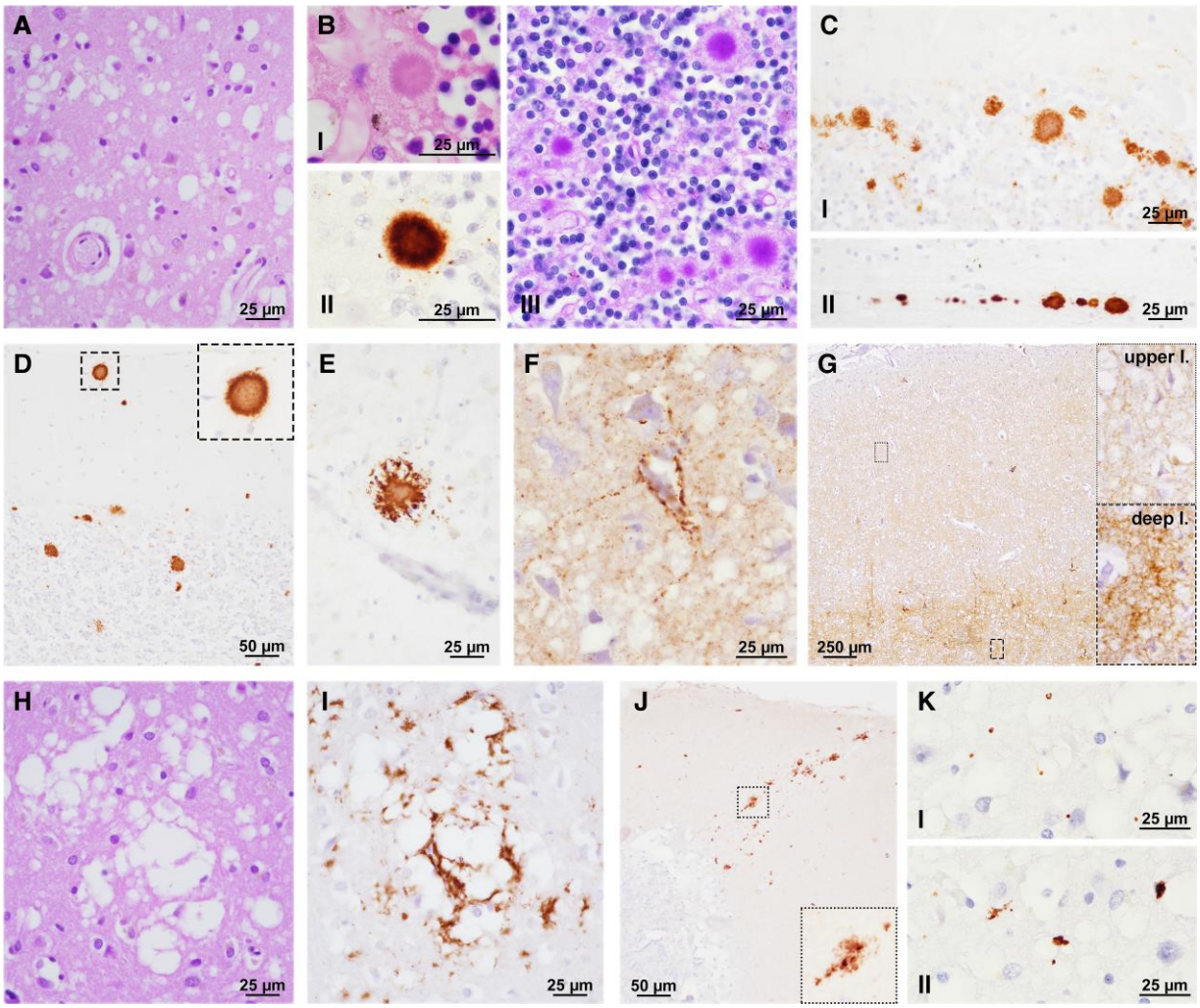

Figure 3 Neuropathologic features of sporadic Creutzfeldt–Jakob disease MV2K subtype. (**A**) Spongiform change with intermediate size vacuoles. (**B**) Cerebellar kuru plaques (**I** = HE; **II** = PrP IHC; **III** = periodic acid-Schiff). (**C**) Plaque-like deposits in the cerebellar granular layer (**I**) and white matter (**II**). (**D**) Kuru plaques in the cerebellar molecular layer and (**E**) occipital cortex. (**F**) Perineuronal PrP and (**G**) deep laminar synaptic staining in neocortex. (**H**) Large size, confluent vacuoles. (**I**) Coarse/perivacuolar PrP deposition. (**J**) Patchy PrP deposits in the cerebellar molecular layer. (**K**) Prion-related tau secondary tauopathy (**I** = dots; **II** = small irregular aggregates). **B**(I), **C**–**G**, **I** and **J**: PrP immunohistochemistry with the mAb 3F4; **K**: tau immunohistochemistry with the mAb AT8.

Table 1 Patterns of PrP deposition

	n	Kuru plaques	Plaque-like	Synaptic	Coarse/perivacuolar
Cerebellum	63	63 (100)	63 (100)	47 (74.6)	0 (0.0)
Neocortex	67	10 (14.9)	63 (94.0)	64 (95.5)	24 (35.8)
Striatum	63	4 (6.3)	63 (100)	60 (95.2)	4 (6.3)
Thalamus	58	6 (10.3)	58 (100)	58 (100)	1 (1.7)
Hypothalamus	45	0 (0.0)	45 (100)	43 (95.5)	(0.0)
Brainstem	57	0 (0.0)	57 (100)	57 (100)	(0.0)
Midbrain	45	0 (0.0)	45 (100)	44 (97.8)	(0.0)
Pons	40	0 (0.0)	40 (100)	38 (95.0)	(0.0)
Medulla oblongata	42	0 (0.0)	39 (92.9)	41 (97.6)	(0.0)

Data are expressed as *n* (%).

disease onset was characterized by bilateral sensory disturbances; dysesthesia was the only presenting symptom in three. Finally, parkinsonism and limb dystonia, often unilateral, mimicking corticobasal degeneration, represented a rare, unusual clinical presentation.

During the early disease stage (i.e. within 6 months from onset), about 80% of MV2K patients showed both cerebellar and cognitive symptoms. Behavioural and psychiatric symptoms were also common, being reported in nearly half of them. As the disease progressed, usually within 12 months after the onset, patients

Table 2 Clinical symptoms at onset and during early stages in 126 patients

Symptoms at onset, n[a]	Percentage (%)	Early symptoms (≤6 months), n[b]	Percentage (%)
Gait/postural unsteadiness, 70 (isolated in 24 cases)	55.5	Gait/postural unsteadiness, 95	75.4
Loss of intellectual abilities,[c] 30 (isolated in 10 cases)	23.8	Loss of intellectual abilities, 86	68.3
Confusion/disorientation, 19	15.1	Behavioural change, 37	29.4
Memory loss (isolated), 18 (isolated in four cases)	14.3	Other psychiatric, 26	20.6
Behavioural changes,[d] 17	13.5	Sleep complaints, 26	20.6
Sleep complaints (hypersomnia, insomnia), 15	11.9	Confusion/disorientation, 25	19.8
Other psychiatric (delirium, hallucinations), 14	11.1	Dysarthria, 17	13.5
Vertigo, 7 (isolated in three cases)	5.5	Visual hallucinations, 13	10.3
Limb dysesthesia, 5 (isolated in three cases)	3.9	Limb dysesthesia, 10	7.9
Dysarthria, 4	3.2	Parkinsonism, 9	7.1
Limb incoordination, 3	2.4	Myoclonus, 9	7.1
Parkinsonism, 3	2.4	Vertigo, 7	5.6
Diplopia, 2	1.6	Limb incoordination, 7	5.6
Transient loss of consciousness, 2	1.6	Diplopia, 5	4.0
Limb dystonia, 2	1.6		

[a]Isolated onset is specified for symptoms occurring at least in three cases.
[b]Only symptoms occurring in at least five cases are reported.
[c]Loss of intellectual abilities includes attention deficit, slow thinking and multiple-domain cognitive dysfunction.
[d]Behavioural changes include one or more of the following: apathy, aboulia, psychomotor agitation, aggressiveness, irritability and oddness.

developed a variable combination of parkinsonism, pyramidal signs, full-blown dementia and myoclonus (Supplementary Fig. 4). As for other disease subtypes, akinetic mutism characterized the end stage of the disease.

The clinical phenotype and disease course were similar in pure MV2K and mixed MV2K + 2C subgroups except for a higher prevalence of parkinsonism in pure MV2K (Supplementary Fig. 5). This finding was independent of the extent of pathologic change in substantia nigra (Fig. 2H). Notably, six out of seven (85.7%) of MV2K + 2C subjects showing perivacuolar/coarse PrP deposits in all neocortices developed cognitive impairment within 6 months from clinical onset, suggesting that the M2C component could have contributed (at least in part) to such clinical presentation.

We investigated the spectrum of possible alternative diagnoses in 119 cases. In most cases, the diagnosis was challenging at first evaluation, especially in early disease stages. As a result, incorrect diagnostic formulations occurred in ∼40% of cases. Neurodegenerative diseases, particularly atypical Alzheimer's disease and cerebellar paraneoplastic disorders, were the most frequent alternative diagnoses. Of note, despite being less common, in a few cases, peripheral polyneuropathy was suspected (Table 3).

Diagnostic investigations

CSF analyses

Prion RT-QuIC

As for inclusion criteria, all probable MV2K were tested positive by either PQ- or IQ-CSF. In those with a definite diagnosis, we detected prion seeding activity in 35 out of 37 tested CSF (94.6%). In both probable and definite cohorts, sensitivity was significantly higher using IQ- than PQ-CSF (63/64, 98.4% versus 51/65, 78.5%, $P < 0.001$). This result was confirmed when limiting the analysis to 53 cases tested by both assays (98.1 versus 75.5%, $P < 0.001$).

Protein 14-3-3

The detection of protein 14-3-3 in CSF demonstrated a suboptimal sensitivity being positive in 51 out of 97 tested patients (52.6%). We found no differences between definite and probable MV2K groups (55.2 versus 48.7%, $P = 0.53$) (Supplementary Table 5).

We did not find either clinical or demographic features to explain the negative 14-3-3 protein results. As the only significant association, as expected, subjects with a positive 14-3-3 finding also showed higher t-tau levels than those 14-3-3 negative (t-tau cut-off >1250 pg/ml: 90.7 versus 60%, $P = 0.004$).

Diffusion-weighted MRI

Brain MRI including FLAIR and DW sequences, demonstrated a high diagnostic sensitivity being positive in 92.2% of tested patients (71/77), with no differences between probable and definite groups (Supplementary Table 5). The most affected brain region on MRI was the striatum, while neocortices showed high-intensity signals in about half of the cases. Interestingly, in participants with a definite diagnosis, hyperintense signals in the neocortex were more common in MV2K + 2C than in MV2K, probably because of the more pronounced cortical spongiform change (Supplementary Fig. 6). One-third of MRIs also revealed abnormal signals in the thalamus; about 15% showed hyperintensities in the limbic system. Overall, subcortical grey nuclei and limbic neocortices were more commonly affected in the pure than in the mixed phenotype (Table 4).

As for 14-3-3 protein, we did not find predictors for negative DW-MRIs. Nonetheless, subjects with negative DW-MRI results showed a trend towards a longer disease duration as compared with those with typical imaging (18.5 (18.0–22.8) versus 13.0 (11.0–18.0) months, $P = 0.059$). Besides, the timing of the investigation was slightly delayed (10 (6.8–15.0) versus 7.0 (4.5–9.0) months, $P = 0.108$). Remarkably, three out of six DW-MRI negative participants had non-diagnostic hyperintensities involving the frontal cortex ($n = 3$), the cingulate gyrus ($n = 2$) and the thalamus ($n = 1$).

EEG

EEG recordings performed in 115 subjects showed a diffuse, non-specific slowing in most cases ($n = 90$, 78.3%), PSWCs in 10 (8.7%) and paroxysmal discharges in two (1.7%). EEG was unremarkable

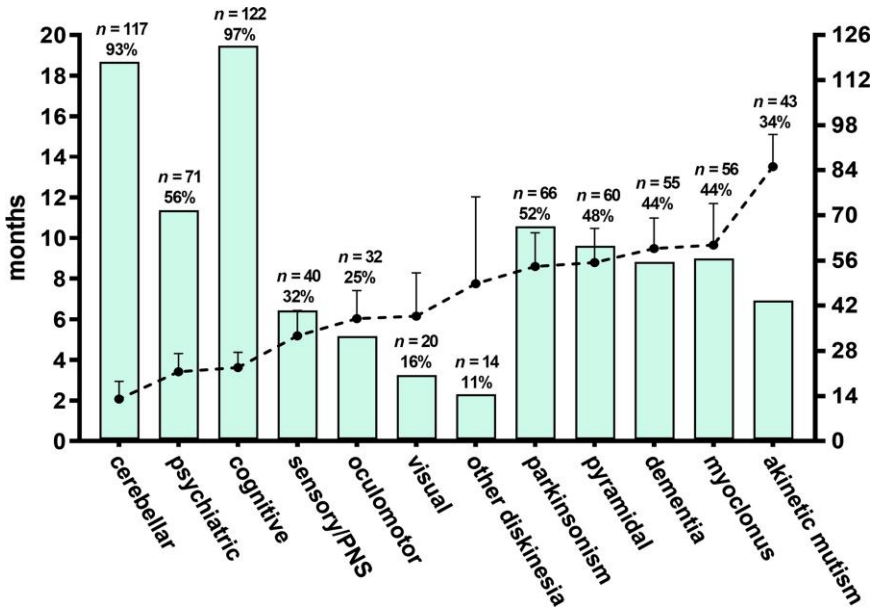

Figure 4 Clinical course of sporadic Creutzfeldt–Jakob disease MV2K subtype. The dashed line indicates the mean time of appearance (in months) from disease onset while bars the frequency for each group of symptoms/signs.

Table 3 Differential diagnosis in 119 patients

Non-CJD diagnoses at first evaluation	*n* (%)
Alzheimer's disease	12 (10.1)
Autoimmune/paraneoplastic syndrome	11 (9.2)
Cerebrovascular disease	6 (5.0)
Lewy body disease	4 (3.4)
Frontotemporal lobar degeneration	3 (2.5)
Peripheral polyneuropathy	3 (2.5)
Wernicke's syndrome	2 (1.7)
Wilson's disease	2 (1.7)
Spinocerebellar ataxia	1 (0.8)
Vestibular disease	1 (0.8)
Amyotrophic lateral sclerosis (bulbar)	1 (0.8)
Cancer	1 (0.8)
Spastic paraparesis	1 (0.8)
Leigh's syndrome	1 (0.8)
Psychiatric	1 (0.8)
Spectrum of all alternative diagnoses[a]	
Neurodegenerative	24 (20.2)
Alzheimer's disease	15 (12.6)
Frontotemporal lobar degeneration	5 (4.2)
Lewy body disease	4 (3.4)
Autoimmune/paraneoplastic	21 (17.6)
Toxic/metabolic	8 (6.7)
Wilson's disease	5 (4.2)
Wernicke's syndrome	3 (2.5)
Vascular	8 (6.7)
Other	9 (7.6)
Spinocerebellar ataxia	6 (5.0)
Peripheral polyneuropathy	3 (2.5)

[a]Only diagnoses reported at least three times were included.

in 13 cases (11.3%). Analysis of timing revealed that normal EEGs were usually recorded during the early disease stage (5.8 ± 2.8 months), whereas PSWCs appeared later in the disease course (9.0 ± 3.8 months).

Table 4 MRI findings in sporadic Creutzfeldt–Jakob disease MV2K

	Overall MV2K[a]	Definite MV2K	Definite MV2K + 2C
n	77	24	18
Positive examination (typical)	71 (92.2)	22 (91.7)	17 (94.4)
Topographic distribution of hyperintensities[b]			
Striatum	58 (81.6)	21 (95.5)	14 (82.4)
Neocortices[c]	35 (49.3)	4 (18.2)	11 (64.7)
Temporal	33 (46.5)	5 (22.7)	10 (58.8)
Parietal	37 (52.1)	4 (18.2)	11 (64.7)
Occipital	35 (49.3)	5 (22.7)	11 (64.7)
Thalamus	24 (33.8)	9 (40.9)	5 (29.4)
Limbic	11 (15.5)	6 (27.3)	0 (0.0)
Hippocampus	5 (7.0)	4 (18.2)	–
Insula	5 (7.0)	2 (9.1)	–
Cingulate gyrus	3 (4.2)	1 (4.5)	–
Timing (months)	7.0 ± 3.3	7.2 ± 3.4	7.4 ± 3.9

Only the examinations including DWI and/or FLAIR sequences were included. Positive examination was defined according to revised diagnostic sporadic Creutzfeldt–Jakob disease criteria.[25]
[a]Includes both definite and probable cases.
[b]Frequencies were calculated only for typical cases.
[c]Isolated hyperintensities were found in the temporal (*n* = 1), parietal (*n* = 4) and occipital cortex (*n* = 3). Additionally, frontal neocortex showed hyperintensities in 31 cases.

Other surrogate biomarkers of neurodegeneration

Overall, CSF t-tau showed higher levels in MV2K patients than non-neurodegenerative controls (Supplementary Fig. 7). Still, compared with the most common MM1 subtype, the extent of this increase was only mild to moderate. After setting a cut-off discriminative of Creutzfeldt–Jakob disease at >1250 pg/ml,[22] we correctly identified 46 out of 60 cases (76.7%). Therefore, t-tau showed greater

sensitivity than 14-3-3 protein ($P = 0.003$) in MV2K. Remarkably, t-tau levels seem to be influenced by the timing of CSF collection; indeed, in all five cases (from the probable group) that underwent serial lumbar puncture over time, the biomarker invariably showed higher values in the last collected sample.

CSF and plasma NfL were analysed in 66 and 24 patients, respectively. The levels of NfL were significantly increased compared with controls in both fluids. In contrast to 14-3-3 and t-tau, they did not differ significantly from those of the MM1 group.

Diagnostic sensitivity of the clinical/biomarker combination criteria

The C-QuIC criterion demonstrated 100% sensitivity even during the early disease stage (Supplementary Table 6). Among the other criteria, C-MRI had higher sensitivity than C-Tau and C-14-3-3 criteria at any time. Remarkably, the sensitivity of all criteria but the C-QuIC one significantly increased when the clinical evaluation accounted for the whole disease course.

Discussion

By focusing on the largest cohort of MV2K, the third most prevalent disease subtype,[3] the present results add to previous studies on the clinical and histo-molecular heterogeneity of Creutzfeldt–Jakob disease, the most common human prion disease. Overall, our results further define MV2K as a highly divergent phenotype, clinically distinguishable from the typical prevalent MM1 that represents the clinical paradigm of sporadic Creutzfeldt–Jakob disease. Moreover, they further underline the high value of both CSF RT-QuIC assay and brain DW-MRI in the clinical diagnosis of MV2K and the relatively low sensitivity of EEG and CSF proteins 14-3-3 and t-tau assays.

Transmission studies have linked the MV2K and VV2 subtypes to the same prion strain (i.e. V2)[4]. The VV2 subtype manifests a short (mean 6.5 months) disease course characterized by early and prominent ataxia and late dementia, reflecting an 'ascending' progression from the cerebellum, brainstem and deep grey nuclei to the neocortices.[5] Conversely, the MV2K subtype shows a slower progression and higher clinical heterogeneity, especially at the onset and early disease stages, probably reflecting a more widespread CNS involvement at symptom onset. Accordingly, our results indicate the early association between progressive cognitive impairment and cerebellar signs as the most frequent clinical presentation, which should raise the suspicion of MV2K, especially in patients with a slower progression than in typical Creutzfeldt–Jakob disease. However, cognitive complaints can be the primary clinical finding in a subgroup of patients, challenging the differential diagnosis with other more prevalent neurodegenerative dementias. Finally, unusual presentations, such as sensory symptoms, vigilance/sleep complaints and unilateral limb dystonia mimicking corticobasal degeneration, may also challenge the early diagnosis and should be considered.[30–32]

The comparison of lesion profiles between VV2 and MV2K reveals a more consistent cortical involvement in the latter. Still, similarly to the VV2 subtype, the neocortical pathology increases according to disease duration in MV2K, indicating that in both subtypes, the cerebellum and other subcortical structures (striatum, thalamus and brainstem) are affected earlier than the cerebral neocortex and that the pathology spreads following a caudal to rostral trajectory. Moreover, the amygdala and hippocampus, part of the limbic system, are also involved early in MV2K. This could explain the relatively high prevalence of psychiatric symptoms and memory deficits at this disease stage.

Both subtypes accumulate PrP in the form of plaque-like deposits. Still, cerebellar kuru plaques have been found only in MV2K, representing the histopathologic hallmark of this subtype due to the V2 strain conversion of PrP129M.

Regarding the PrP^{Sc} typing, the immunoblot profile of the unglycosylated PrP^{Sc} comprises a doublet at 20 and 19 kDa instead of a unique band at 19 kDa representing another significant difference between MV2K and VV2. Again, the difference reflects the conversion of both PrP129M (20 kDa band) and 129V (19 kDa band). Here we demonstrated that the relative amount of the two bands is region dependent: in the thalamus, striatum and cerebellum, the 20-kDa band is usually more prominent or isointense, while the 19 kDa fragment predominates in the neocortices.

We also confirmed the influence of PrP129M conversion on the histo-molecular phenotype, demonstrating the association between the number of kuru plaques and the relative amount of 20 kDa PrP^{Sc} fragment in the cerebellum.

Of note, several of the MV2K features, including the relatively slow progression, the reduced expression of the 20 kDa fragment in the neocortices whose involvement depends on disease duration, and the association between the number of kuru plaques and disease duration might rely on the less efficient conversion of PrP129M. Indeed, transmission studies in mice expressing different forms of the human *PRNP* gene showed that the V2 strain manifests a higher attack rate and a shorter incubation period in the mice carrying 129VV compared to those with 129MV,[4,6] which explains well the VV2 and MV2K discrepancies.

On another relevant issue, codon 129 heterozygosis makes these patients more permissive to the co-existence of multiple strains within the same brain. Indeed, the co-expression of both PrP129M and PrP129V expands the possible conformations that the disease-associated misfolded PrP may acquire. The most common subtype associated with MV2K was MV2C (e.g. strain M2C). Despite the relevance from a biological standpoint, in our cohort, the mixed MV2K + 2C phenotype had a modest impact on the clinical phenotype and results of diagnostic investigations. These findings could be explained by the focal distribution of the non-dominant histotype/strain (M2C), often limited to the occipital cortex. However, that a more widespread M2C co-occurrence might have a more substantial impact on the clinical phenotype cannot be excluded. Indeed, six out of seven cases in which we detected MV2C features in all neocortices presented with early cognitive symptoms.

For the diagnosis in vitam, besides the atypical long disease course, physicians should also be aware that the accuracy of the available diagnostic tests for Creutzfeldt–Jakob disease varies significantly. This is particularly true for subtypes with more prolonged duration, such as the MV2K. In particular, the prion RT-QuIC showed an overall high sensitivity (~95%), mainly when the protocol with truncated (90–231) recombinant PrP was used (98%). By contrast, the sensitivity was only suboptimal using the first-generation RT-QuIC (full-length PrP) (79%). In line with these findings, in case of a negative RT-QuIC response, knowing the assay protocol used by the laboratory would be critical to interpreting the result correctly. Applying current MRI criteria,[25] DW-MRI also showed a high sensitivity (91%). This result has high relevance considering that the assessed MRIs were, in most cases, evaluated by general neuroradiologists not trained explicitly in the Creutzfeldt–Jakob disease diagnosis. In the overall cohort, typical hyperintensities involved the striatum more frequently than

neocortices, the latter being significantly more common in MV2K + 2C cases. Notably, the thalamus in about a third of patients and the limbic system in some cases (~15%) also showed hyperintense signals.[33] These findings are consistent with the regional lesion profile, particularly the spongiform change distribution.[34]

In contrast with the most prevalent MM1 and VV2 subtypes, CSF surrogate biomarkers of neuronal degeneration, such as 14-3-3 and t-tau proteins, had low sensitivity in MV2K, resulting in poor diagnostic utility. Therefore, physicians should not rule out the diagnosis of sporadic Creutzfeldt–Jakob disease (MV2K subtype) in cases testing CSF 14-3-3 negative or showing t-tau levels below the cut-off value supporting the diagnosis of CJD. The moderate increase of t-tau and 14-3-3 proteins in the CSF of MV2K patients compared with those with MM1 and VV2 indicates lower toxicity of amyloid PrP aggregates in this condition.[35,36] Of note, the brain area showing the highest difference in the severity of neurodegenerative changes between VV2 and MV2K is the cerebellum, the region with the amyloid plaques of the kuru type and the most abundant plaque-like deposits.[37]

Similarly, Gerstmann–Sträussler–Scheinker disease, a genetic prion disease characterized by extracellular aggregation and accumulation of PrP forming amyloid plaques, typically manifests a slow progression and an overall disease duration of several years.[38] Altogether, these observations support the current view of reduced neurotoxicity of large protein aggregates forming amyloid plaques compared to small dispersed aggregates such as oligomers in neurodegenerative diseases.

Unlike 14-3-3 and t-tau, NfL, a marker of neuro-axonal injury, increases significantly in MV2K, showing levels in CSF comparable with those in MM1. Therefore, in cases with suspected MV2K, evaluating NfL levels could be useful, especially in those testing negative for 14-3-3 and t-tau, to support the suspicion of MV2K.[24,39] Additionally, NfL can be accurately measured in plasma, allowing for longitudinal analyses of disease progression and therapeutic response monitoring.[40–42] Finally, we included in the present study a consecutive cohort of 'probable' MV2K selected by applying the following criteria: (i) MV genotype at codon 129; (ii) disease duration >8 months; and (iii) clinical evidence of cerebellar and/or nigrostriatal involvement within 6 months from the onset. The clinical features and results of diagnostic investigations did not differ between probable and definite MV2K cases, suggesting that by combining the determination of codon 129 genotype and stringent clinical criteria, a specific, accurate diagnosis of MV2K can be reached in vitam in most cases (Supplementary Fig. 8). Future studies on large sporadic Creutzfeldt–Jakob cohorts including all disease subtypes are required to confirm the accuracy of the proposed diagnostic algorithm.

Strengths of our work included the comprehensive clinical, neuropathological and molecular characterization in the most extensive MV2K case series reported to date. The main limits of the study are the retrospective nature of the clinical characterization of probable cases and the lack of a systematic revision of brain MRIs by experienced neuroradiologists.

Conclusion

In summary, MV2K is the most common 'atypical' subtype of sporadic Creutzfeldt–Jakob disease due to the relatively long disease duration and slow progression and the poor sensitivity of some diagnostic tests such as CSF 14-3-3 protein and EEG. Most clinical heterogeneity relies on the interplay between biological disease determinants (strain) and host factors (genetic), which uniquely bring to PrP accumulation in the form of cerebellar amyloid kuru plaques.

Clinicians should consider MV2K in patients with (or early developing) mixed progressive cognitive and cerebellar dysfunctions. CSF prion RT-QuIC and brain DW-MRI represent the most sensitive diagnostic tests. Altogether these data strongly suggest that, despite some unusual features, MV2K can be diagnosed accurately in vitam based on clinical data, DW-MRI, CSF prion RT-QuIC assay and codon 129 genotyping.

Acknowledgements

The authors wish to thank the numerous Italian neurologists who provided clinical information. We are also in debt to Barbara Polischi, MSc, and Benedetta Carlà, MSc, for their valuable technical assistance. Open access funding provided by Bibliosan.

Funding

This work was financially supported by the Ministero della Salute (RC) and the Università di Bologna (RFO).

Supplementary material

Supplementary material is available at *Brain* online.

Competing interests

The authors report no competing interests.

References

1. Kobayashi A, Teruya K, Matsuura Y, *et al*. The influence of PRNP polymorphisms on human prion disease susceptibility: An update. *Acta Neuropathol*. 2015;130:159-170.
2. Parchi P, Castellani R, Capellari S, *et al*. Molecular basis of phenotypic variability in sporadic Creutzfeldt-Jakob disease. *Ann Neurol*. 1996;39:767-778.
3. Parchi P, Giese A, Capellari S, *et al*. Classification of sporadic Creutzfeldt-Jakob disease based on molecular and phenotypic analysis of 300 subjects. *Ann Neurol*. 1999;46:224-233.
4. Bishop MT, Will RG, Manson JC. Defining sporadic Creutzfeldt-Jakob disease strains and their transmission properties. *Proc Natl Acad Sci USA*. 2010;107:12005-12010.
5. Baiardi S, Magherini A, Capellari S, *et al*. Towards an early clinical diagnosis of sporadic CJD VV2 (ataxic type). *J Neurol Neurosurg Psychiatry*. 2017;88:764-772.
6. Kobayashi A, Iwasaki Y, Otsuka H, *et al*. Deciphering the pathogenesis of sporadic Creutzfeldt-Jakob disease with codon 129 M/V and type 2 abnormal prion protein. *Acta Neuropathol Commun*. 2013;1:74.
7. Nemani SK, Xiao X, Cali I, *et al*. A novel mechanism of phenotypic heterogeneity in Creutzfeldt-Jakob disease. *Acta Neuropathol Commun*. 2020;8:85.
8. Krasnianski A, Schulz-Schaeffer WJ, Kallenberg K, *et al*. Clinical findings and diagnostic tests in the MV2 subtype of sporadic CJD. *Brain*. 2006;129:2288-2296.
9. Kobayashi A, Sakuma N, Matsuura Y, Mohri S, Aguzzi A, Kitamoto T. Experimental verification of a traceback phenomenon in prion infection. *J Virol*. 2010;84:3230-3238.

10. Parchi P, Strammiello R, Notari S, *et al*. Incidence and spectrum of sporadic Creutzfeldt-Jakob disease variants with mixed phenotype and co-occurrence of PrPSc types: An updated classification. *Acta Neuropathol*. 2009;118:659-671.
11. Heinemann U, Krasnianski A, Meissner B, *et al*. Creutzfeldt-Jakob disease in Germany: A prospective 12-year surveillance. *Brain*. 2007;130:1350-1359.
12. Nozaki I, Hamaguchi T, Sanjo N, *et al*. Prospective 10-year surveillance of human prion diseases in Japan. *Brain*. 2010;133: 3043-3057.
13. Jansen C, Parchi P, Capellari S, *et al*. Human prion diseases in the Netherlands (1998–2009): Clinical, genetic and molecular aspects. *PLoS One*. 2012;7:e36333.
14. Parchi P, Notari S, Weber P, *et al*. Inter-laboratory assessment of PrPSc typing in Creutzfeldt-Jakob disease: A western blot study within the NeuroPrion Consortium. *Brain Pathol*. 2009;19: 384-391.
15. Parchi P, de Boni L, Saverioni D, *et al*. Consensus classification of human prion disease histotypes allows reliable identification of molecular subtypes: An inter-rater study among surveillance centres in Europe and USA. *Acta Neuropathol*. 2012;124: 517-529.
16. Baiardi S, Rossi M, Mammana A, *et al*. Phenotypic diversity of genetic Creutzfeldt-Jakob disease: A histo-molecular-based classification. *Acta Neuropathol*. 2021;142:707-728.
17. Notari S, Capellari S, Langeveld J, *et al*. A refined method for molecular typing reveals that co-occurrence of PrP(Sc) types in Creutzfeldt-Jakob disease is not the rule. *Lab Invest*. 2007;87: 1103-1112.
18. Rossi M, Saverioni D, Di Bari M, *et al*. Atypical Creutzfeldt-Jakob disease with PrP-amyloid plaques in white matter: Molecular characterization and transmission to bank voles show the M1 strain signature. *Acta Neuropathol Commun*. 2017;5:87.
19. Thal DR, Rüb U, Orantes M, Braak H. Phases of A beta-deposition in the human brain and its relevance for the development of AD. *Neurology*. 2002;58:1791-1800.
20. Alafuzoff I, Arzberger T, Al-Sarraj S, *et al*. Staging of neurofibrillary pathology in Alzheimer's disease: A study of the BrainNet Europe Consortium. *Brain Pathol*. 2008;18:484-496.
21. Alafuzoff I, Ince PG, Arzberger T, *et al*. Staging/typing of Lewy body related alpha-synuclein pathology: A study of the BrainNet Europe Consortium. *Acta Neuropathol*. 2009;117: 635-652.
22. Lattanzio F, Abu-Rumeileh S, Franceschini A, *et al*. Prion-specific and surrogate CSF biomarkers in Creutzfeldt-Jakob disease: Diagnostic accuracy in relation to molecular subtypes and analysis of neuropathological correlates of p-tau and Aβ42 levels. *Acta Neuropathol*. 2017;133:559-578.
23. Franceschini A, Baiardi S, Hughson AG, *et al*. High diagnostic value of second generation CSF RT-QuIC across the wide spectrum of CJD prions. *Sci Rep*. 2017;7:10655.
24. Abu-Rumeileh S, Baiardi S, Polischi B, *et al*. Diagnostic value of surrogate CSF biomarkers for Creutzfeldt-Jakob disease in the era of RT-QuIC. *J Neurol*. 2019;266:3136-3143.
25. Zerr I, Kallenberg K, Summers DM, *et al*. Updated clinical diagnostic criteria for sporadic Creutzfeldt-Jakob disease. *Brain*. 2009;132:2659-2668.
26. Wieser HG, Schindler K, Zumsteg D. EEG in Creutzfeldt-Jakob disease. *Clin Neurophysiol*. 2006;117:935-951.
27. Abu-Rumeileh S, Steinacker P, Polischi B, *et al*. CSF biomarkers of neuroinflammation in distinct forms and subtypes of neurodegenerative dementia. *Alzheimers Res Ther*. 2019;12:2.
28. Montine TJ, Phelps CH, Beach TG, *et al*. National institute on aging-Alzheimer's association guidelines for the neuropathologic assessment of Alzheimer's disease: A practical approach. *Acta Neuropathol*. 2012;123:1-11.
29. Crary JF, Trojanowski JQ, Schneider JA, *et al*. Primary age-related tauopathy (PART): A common pathology associated with human aging. *Acta Neuropathol*. 2014;128:755-766.
30. Magherini A, Pentore R, Galassi G, Stucchi CM, Capellari S, Parchi P. MV2 Subtype of sporadic Creutzfeldt-Jakob disease presenting as corticobasal syndrome. *Mov Disord*. 2007;22: 898-899.
31. Baiardi S, Capellari S, Bartoletti Stella A, Parchi P. Unusual clinical presentations challenging the early clinical diagnosis of Creutzfeldt-Jakob disease. *J Alzheimers Dis*. 2018;64:1051-1065.
32. Wu HM, Lu CS, Huang CC, *et al*. Asymmetric involvement in sporadic Creutzfeldt-Jakob disease: Clinical, brain imaging, and electroencephalographic studies. *Eur Neurol*. 2010;64:74-79.
33. Pascuzzo R, Oxtoby NP, Young AL, *et al*. Prion propagation estimated from brain diffusion MRI is subtype dependent in sporadic Creutzfeldt-Jakob disease. *Acta Neuropathol*. 2020;140: 169-181.
34. Manners DN, Parchi P, Tonon C, *et al*. Pathologic correlates of diffusion MRI changes in Creutzfeldt-Jakob disease. *Neurology*. 2009;72:1425-1431.
35. Caughey B, Lansbury PT. Protofibrils, pores, fibrils, and neurodegeneration: Separating the responsible protein aggregates from the innocent bystanders. *Annu Rev Neurosci*. 2003;26:267-298.
36. Corsaro A, Thellung S, Villa V, Nizzari M, Florio T. Role of prion protein aggregation in neurotoxicity. *Int J Mol Sci*. 2012;13: 8648-8669.
37. McLean CA, Ironside JW, Alpers MP, *et al*. Comparative neuropathology of Kuru with the new variant of Creutzfeldt-Jakob disease: Evidence for strain of agent predominating over genotype of host. *Brain Pathol*. 1998;8:429-437.
38. Ghetti B, Piccardo P, Zanusso G. Dominantly inherited prion protein cerebral amyloidoses—A modern view of Gerstmann-Sträussler-Scheinker. *Handb Clin Neurol*. 2018;153:243-269.
39. Zerr I, Villar-Piqué A, Hermann P, *et al*. Diagnostic and prognostic value of plasma neurofilament light and total-tau in sporadic Creutzfeldt-Jakob disease. *Alzheimers Res Ther*. 2021;13:86.
40. Abu-Rumeileh S, Baiardi S, Ladogana A, *et al*. Comparison between plasma and cerebrospinal fluid biomarkers for the early diagnosis and association with survival in prion disease. *J Neurol Neurosurg Psychiatry*. 2020;91:1181-1188.
41. Thompson AGB, Anastasiadis P, Druyeh R, *et al*. Evaluation of plasma tau and neurofilament light chain biomarkers in a 12-year clinical cohort of human prion diseases. *Mol Psychiatry*. 2021;26:5955-5966.
42. Staffaroni AM, Kramer AO, Casey M, *et al*. Association of blood and cerebrospinal fluid tau level and other biomarkers with survival time in sporadic Creutzfeldt-Jakob disease. *JAMA Neurol*. 2019;76:969-977.